HHS Public Access

Author manuscript

Science. Author manuscript; available in PMC 2024 February 17.

Published in final edited form as:

Science. 2023 February 17; 379(6633): 700–706. doi:10.1126/science.adf0435.

Psychedelics Promote Neuroplasticity Through Activation of Intracellular 5-HT2A Receptors

Maxemiliano V. Vargas[1,2], **Lee E. Dunlap**[2,3,‡], **Chunyang Dong**[4,‡], **Samuel J. Carter**[2,3], **Robert J. Tombari**[2,3], **Shekib A. Jami**[5], **Lindsay P. Cameron**[1], **Seona D. Patel**[3], **Joseph J. Hennessey**[6], **Hannah N. Saeger**[2,7], **John D. McCorvy**[6], **John A. Gray**[2,5,8], **Lin Tian**[2,5,9], **David E. Olson**[2,3,5,9,*]

[1]Neuroscience Graduate Program, University of California, Davis; Davis, CA 95618, USA.

[2]Institute for Psychedelics and Neurotherapeutics, University of California, Davis, Davis, CA 95618, USA

[3]Department of Chemistry, University of California, Davis; Davis, CA 95616, USA.

[4]Biochemistry, Molecular, Cellular, and Developmental Biology Graduate Program, University of California, Davis; Davis, CA 95616, USA.

[5]Center for Neuroscience, University of California, Davis; Davis, CA 95618, USA.

[6]Department of Cell Biology, Neurobiology, and Anatomy, Medical College of Wisconsin; Milwaukee, WI 53226, USA

[7]Pharmacology and Toxicology Graduate Program, University of California, Davis; Davis, CA 95616, USA.

[8]Department of Neurology, School of Medicine, University of California, Davis, Sacramento, CA 95817, USA

[9]Department of Biochemistry & Molecular Medicine, School of Medicine, University of California, Davis; Sacramento, CA 95817, USA.

Abstract

[*]Corresponding author. deolson@ucdavis.edu.
[‡]Equal Contributions

Author contributions. MVV performed the majority of the in vitro experiments including the dendritogenesis, spinogenesis, subcellular colocalization, IP1, neuromics antibody validation, and psychLight assays. CD performed the surgeries as well as the perfusions. MVV performed the brain slice imaging with assistance from CD. MVV performed the behavioral experiments. LED performed the N-methylation SAR dendritogenesis experiments, calculated cLogP values, and synthesized TMT and MKTSN. RJT and SC performed the radioligand binding studies. HNS performed culturing of 5-HT2AR KO cultures. LPC and SDP performed the Golgi staining experiments. SAJ performed the electrophysiology experiments. JJH performed BRET assays of 5-HT2AR activation. JDM, JAG, LT, and DEO supervised various aspects of this project and assisted with data analysis. DEO conceived the project and wrote the manuscript with input from all authors.

Competing Interests. DEO is a co-founder of Delix Therapeutics, Inc., serves as the Chief Innovation Officer and Head of the Scientific Advisory Board, and has sponsored research agreements with Delix Therapeutics. Delix Therapeutics has licensed technology from the University of California, Davis. The sponsors of this research were not involved in the conceptualization, design, decision to publish, or preparation of the manuscript.

Supplementary Materials:
Materials and Methods
Figs S1 to S10
References 57–59

Decreased dendritic spine density in the cortex is a hallmark of several neuropsychiatric diseases, and the ability to promote cortical neuron growth has been hypothesized to underlie the rapid and sustained therapeutic effects of psychedelics. Activation of serotonin 2A receptors (5-HT2ARs) is essential for psychedelic-induced cortical plasticity, but it is currently unclear why some 5-HT2AR agonists promote neuroplasticity while others do not. Here, we use molecular and genetic tools to demonstrate that intracellular 5-HT2ARs mediate the plasticity-promoting properties of psychedelics—results that explain why serotonin does not engage similar plasticity mechanisms. This work emphasizes the role of location bias in 5-HT2AR signaling, identifies intracellular 5-HT2ARs as a new therapeutic target, and raises the intriguing possibility that serotonin might not be the endogenous ligand for intracellular 5-HT2ARs in the cortex.

One Sentence Summary:

Membrane permeable psychedelics promote cortical neuron growth by activating intracellular 5-HT2A receptors.

Dysregulation of the cortex has been hypothesized to play a significant role in the pathophysiology of mental illnesses such as depression and often manifests as structural changes including decreased dendritic arbor complexity and reduced dendritic spine density (1,2,3). Traditional antidepressants, such as selective serotonin reuptake inhibitors (SSRIs), can rescue these deficits following chronic treatment, though it seems that their effects may be independent of serotonin and perhaps involve activation of tropomyosin receptor kinase B (TrkB) signaling (4,5). A new class of therapeutic compounds known as psychoplastogens (6) are differentiated from SSRIs by their ability to produce both rapid and sustained effects on structural plasticity and behavior following a single administration (7). Psychoplastogens include both ketamine and serotonergic psychedelics, though their primary targets are distinct (7).

Psychedelics are serotonin 2A receptor (5-HT2AR) agonists that can lead to profound changes in perception, cognition, and mood (8). Recent evidence suggests that they promote cortical structural and functional neuroplasticity via activation of 5-HT2ARs (9,10). The mechanism by which 5-HT2AR activation leads to changes in neuronal growth is still poorly defined, though it appears to involve TrkB, mTOR, and AMPA receptor signaling (11). It is currently unclear why some 5-HT2AR ligands can promote neuroplasticity and produce sustained therapeutic behavioral responses in the absence of hallucinogenic effects, while other 5-HT2AR agonists do not promote plasticity at all (12,13,14,15). In fact, serotonin itself does not produce psychedelic-like effects on neuronal growth when administered to cortical cultures (9). This enigmatic finding cannot be easily explained by traditional biased agonism, as serotonin is a balanced agonist of the 5-HT2AR, exhibiting high potency and efficacy for activating both G protein and β-arrestin pathways (16, 17).

Unlike psychedelics, the physicochemical properties of serotonin prevent it from entering cells by passively diffusing across nonpolar membranes (8). Thus, we reasoned that another form of functional selectivity, known as location bias, might explain the difference in cellular signaling elicited by serotonin and psychedelics (18,19). Here we leveraged both chemical design and genetic manipulation to test the hypothesis that activation of an

intracellular population of 5-HT2ARs is necessary for 5-HT2AR ligands to induce cortical structural plasticity and produce antidepressant-like behavioral responses.

Lipophilicity correlates with psychoplastogenicity

To firmly establish the role of 5-HT2AR activation in psychedelic-induced spinogenesis, we administered 5-methoxy-*N,N*-dimethyltryptamine (5-MeO) to wild type (WT) and 5-HT2AR knockout (KO) mice (20) and assessed structural and functional changes in layer 5 pyramidal neurons of the prefrontal cortex (PFC) 24 h later (fig. S1A–C). Golgi-Cox staining revealed that 5-MeO increased spine density in both male and female animals, and this effect was absent in 5-HT2AR KO mice (fig. S1A and B). Furthermore, ex vivo electrophysiology confirmed that 5-HT2AR activation is necessary for 5-MeO to produce sustained increases in both the frequency and amplitude of spontaneous excitatory postsynaptic currents (sEPSCs) (fig. S1C).

Next, we determined how the structures of 5-HT2AR ligands impact their abilities to promote neuronal growth by treating embryonic rat cortical neurons with serotonin (5-HT), tryptamine (TRY), 5-methoxytryptamine (5-MeO-TRY) and their corresponding *N*-methyl and *N,N*-dimethyl congeners (Fig. 1A) prior to assessing neuronal morphology via Sholl analysis (21). Ketamine was used as a positive control due to its known ability to induce structural plasticity in this assay (9). These structure-activity relationship (SAR) studies revealed that increasing *N*-methylation led to an enhanced ability to promote neuronal growth with the *N,N*-dimethyl compounds increasing dendritic arbor complexity to the greatest extent (Fig. 1B to D).

Increasing *N*-methylation is known to impact the efficacy of 5-HT2AR signaling, so we attempted to correlate psychoplastogenic efficacy across a range of 5-HT2AR ligands with efficacy in a traditional [^{3}H]-IP accumulation assay (Fig. 1E) (22). Surprisingly, we did not observe a positive correlation between psychoplastogenic effects and ligand efficacy. In fact, there seemed to be a non-significant inverse correlation between [^{3}H]-IP accumulation and dendritogenesis efficacy (Fig. 1E). To avoid potential issues associated with amplification of secondary messengers, we utilized psychLight2—a fluorescent biosensor capable of directly detecting changes in 5-HT2AR conformation (14). PsychLight2 efficacy closely mirrored that observed using [^{3}H]-IP accumulation assays, though psychLight2 efficacy exhibited an even stronger anti-correlation with dendritogenesis efficacy ($p = 0.06$, Fig. 1F). Finally, we employed bioluminescence resonance energy transfer (BRET) assays to directly measure G_q activation or β-arrestin-2 recruitment (fig. S2) (23). Both measures of 5-HT2AR efficacy exhibited a strong negative correlation with psychoplastogenicity (Fig. 1G and H). Moreover, both G_q activation and β-arrestin recruitment correlated well with psychLight efficacy ($R^2 = 0.9$, $p = <0.0001$ and 0.0006, respectively) (Fig. 1I). Negative correlation between 5-HT2AR efficacy and psychoplastogenicity should be interpreted with caution, as this relationship may only apply to tryptamine-based ligands or compounds exhibiting a threshold level of 5-HT2AR activation.

Nitrogen methylation of 5-HT2AR ligands structurally related to serotonin is known to result in partial agonism (22), but it also has a profound effect on their physicochemical

properties. These compounds display a wide range of lipophilicities ranging from highly polar molecules like serotonin to relatively nonpolar compounds like *N,N*-dimethyltryptamine (DMT). Using calculated LogP (cLogP) values, we observed a significant positive correlation with psychoplastogenic effects—more lipophilic agonists exhibited greater abilities to promote structural plasticity than polar compounds (Fig. 1J). This relationship was evident within the TRY, 5-HT, and 5-MeO-TRY scaffolds. The finding that lipophilicity was a better predictor of psychoplastogenicity than 5-HT2AR activation led us to hypothesize that an intracellular pool of 5-HT2ARs in cortical neurons might be responsible for psychedelic-induced neuronal growth.

Primary localization of 5-HT2ARs in Cortical Neurons is Intracellular

While most GPCRs are believed to be localized primarily to the plasma membrane, several exhibit substantial intracellular localization (24,25,26,27). In vitro and ex vivo experiments have also established the existence of large intracellular pools of 5-HT2ARs in various cell types in the absence of a ligand (28,29,30,31). To compare 5-HT2AR localization patterns between cell types, we expressed a Myc-5-HT2A-ECFP construct in both HEK293T cells and cortical neurons, performed live cell imaging, and assessed colocalization with a membrane dye (Cellbrite® Steady) that labels the extracellular side of the plasma membrane. Because overexpression of tagged receptor constructs might alter trafficking and localization, we included several controls. We utilized a β2 adrenergic receptor tagged with ECFP (β2AR-ECFP) as a GPCR that is canonically described as being plasma membrane bound, and we used an ECFP construct to establish the localization of a fluorescent protein that is not tagged to a GPCR (32,33).

When expressed in HEK293T cells cultured in the absence of serum, 5-HT2ARs and β2ARs exhibited similar cellular expression patterns (Fig. 2A) and possessed correlation coefficients with the plasma membrane marker that were not statistically different (Fig. 2B). However, these two GPCRs displayed distinct localization patterns in neurons. In cortical neurons, β2AR expression was more highly correlated with the plasma membrane marker than was 5-HT2AR expression (Fig. 2B), demonstrating that overexpression of a GPCR in cortical neurons doesn't necessarily lead to intracellular localization. The extent of overexpression was similar for 5-HT2ARs and β2ARs in both HEK293T cells and cortical neurons (fig. S3A). We performed these localization experiments without serum in the culturing media because serum contains serotonin, which can lead to agonist-induced changes in trafficking and localization (fig. S3B and C). In both neurons and HEK293T cells, the expression patterns of the tagged GPCRs were markedly distinct from ECFP, confirming that the GPCR component of the constructs dictates cellular localization. Expression of a FLAG-5-HT2AR construct in rat cortical neurons produced a similar intracellular localization pattern, suggesting that these tags do not significantly alter the localization patterns of the 5-HT2AR (34).

Bright punctate staining within neurons suggested that 5-HT2ARs were localized within intracellular compartments (Fig. 2A), so we performed additional immunocytochemistry experiments to assess overlap with markers of various subcellular organelles (fig. S4). We observed a high level of 5-HT2AR colocalization with Rab5 and Rab7 in both HEK293T

cells and neurons. Ras-related GTPases of the Rab family are known to regulate intracellular transport of GPCRs (35). We observed a very large difference in 5-HT2AR colocalization with the Golgi apparatus between neurons and HEK293T cells, with the former exhibiting substantially higher correlation coefficients (fig. S4). The Golgi apparatus is a key regulator of GPCR signaling, and ligands can either passively diffuse into Golgi-localized receptor pools or gain access by facilitated transmembrane transport (18,36 37). Signaling from within the Golgi can be distinct, as is the case for opioid receptors (38).

To ensure that high 5-HT2AR colocalization with the Golgi was not an artifact of overexpression, we assessed native 5-HT2AR expression in neurons using one of the few validated 5-HT2AR antibodies (30). To confirm the antibody's specificity, we performed in-house validation by overexpressing 5-HT2ARs in HEK293T cells (fig. S5A) and utilized mouse 5-HT2AR knockout cortical neurons (fig. S5B). Next, we imaged rat embryonic cortical neurons expressing only native 5-HT2ARs or overexpressing a Myc-5-HT2A-ECFP construct. Longitudinal and transverse line scans indicated that Myc-5-HT2A-ECFP expression closely mirrored the native localization pattern of 5-HT2ARs (fig. S5C and D).

Membrane permeability is required for psychedelic-induced neuroplasticity

Given that cortical neurons possess a large pool of intracellular 5-HT2ARs, we next used chemical tools to determine if activation of this intracellular population was essential for psychedelics to promote structural neuroplasticity. Chemical modification of the membrane permeable ligands DMT, psilocin (PSI), and ketanserin (KTSN) converted them into highly charged membrane impermeable congeners *N,N,N*-trimethyltryptamine (TMT), psilocybin (PSY), and methylated ketanserin (MKTSN), respectively (Fig. 3A). All of the charged species exhibited negative cLogP scores (fig. S6A) but retained affinity for 5-HT2ARs as determined by radioligand competition binding experiments (fig. S6B). In psychLight2 assays, the membrane impermeable analogs displayed comparable efficacies to their uncharged parent molecules with reduced potencies (fig. S6C and D).

Next, we treated freshly dissected rat embryonic cortical neurons with DMT (1 μM) and PSI (1 μM) as well as their membrane impermeable congeners in the presence and absence of electroporation. Electroporation creates temporary openings in the plasma membrane, enabling highly charged molecules to pass through and access the intracellular space. While the membrane permeable 5-HT2AR agonists were able to promote dendritogenesis regardless of whether or not electroporation was applied, the membrane impermeable compounds could only promote neuronal growth when applied with electroporation (Fig. 3B and C). Similarly, the membrane permeable 5-HT2AR antagonist KTSN (treated in ten-fold excess at 10 μM) blocked DMT-induced plasticity both with and without electroporation; however, the membrane impermeable antagonist MKTSN (10 μM) could only block DMT-induced neuronal growth when it was applied with electroporation (Fig. 3B and C). Using more mature neurons (DIV15), we demonstrated that the membrane permeable 5-HT2AR agonists increased dendritic spine density—another measure of structural neural plasticity—while the membrane-impermeable agonists did not (Fig. 3D and E). KTSN was able to inhibit the effects of DMT and PSI on dendritic spine density while MKTSN was not (fig. S7).

To further establish that membrane permeable and impermeable ligands target different populations of 5-HT2ARs, we performed an experiment in HEK293T cells expressing psychLight1. The psychLight1 construct was chosen over psychLight2 because the former lacks an ER export sequence, resulting in greater intracellular localization (14). PsychLight1 expressing HEK293T cells were pretreated with either vehicle or MKTSN to selectively antagonize the population of 5-HT2ARs expressed on the plasma membrane. Next, changes in psychLight1 fluorescence were measured following administration of the membrane impermeable ligand serotonin or its membrane permeable congener 5-MeO-DMT. As serotonin is a full agonist, it induced a stronger response in the absence of antagonist compared to the partial agonist 5-MeO-DMT. Pretreatment with MKTSN resulted in a much larger reduction in the serotonin-induced psychLight1 signal compared to that induced by 5-MeO-DMT (Fig. 3F). Pretreatment with MKTSN could nearly fully antagonize the effect of serotonin. In sharp contrast, MKTSN only partially blocked the ability of 5-MeO-DMT to turn on psychLight1 fluorescence.

Because serotonin and 5-MeO-DMT exhibit different lipophilicities (cLogP values of 0.57 and 2.33, respectively), we reasoned that their abilities to displace [^{3}H]-LSD bound to the 5-HT2AR would depend on whether those receptors were exposed to the extracellular environment. Thus, we performed radioligand competition binding experiments using intact HEK293T cells expressing Myc-5-HT2AR or psychLight2 as well as membrane preparations obtained from these systems. The K_i values for serotonin and 5-MeO-DMT were nearly identical when utilizing membrane preparations or intact PSYLI2 cells—HEK293T cells stably expressing a 5-HT2AR construct with an ER export sequence resulting in a large proportion of the 5-HT2ARs being exposed to the extracellular environment (fig. S8). However, 5-MeO-DMT was an order of magnitude more potent than serotonin when using intact HEK293T cells expressing large populations of both plasma membrane bound and intracellular 5-HT2ARs (fig. S8).

To confirm that serotonin and 5-MeO-DMT can target distinct populations of 5-HT2ARs, we performed IP1 assays in both cortical neurons and HEK293T cells expressing the Myc-5-HT2A-ECFP construct. When the assay was performed in Myc-5-HT2A-ECFP expressing HEK293T cells, which display a large proportion of plasma membrane bound 5-HT2ARs, serotonin and 5-MeO-DMT had comparable potencies and efficacies (fig. S9A). When the same experiment was performed in rat cortical neurons, serotonin failed to elicit an agonist response, though 5-MeO-DMT remained a potent agonist (fig. S9B).

Cellular import of serotonin leads to structural plasticity and antidepressant-like effects

If activation of intracellular 5-HT2ARs in cortical neurons is sufficient to promote structural plasticity, we hypothesized that serotonin should be able to promote cortical neuron growth if given access to the intracellular space. To test this hypothesis, we first treated cortical neurons with 5-HT (1 μM) in the presence and absence of electroporation. Unlike ketamine (1 μM), 5-HT was only able to promote cortical neuron growth when applied with electroporation (Fig. 4A). Next, we took advantage of the serotonin transporter (SERT),

which can import serotonin from the extracellular environment (39). Endogenous expression of SERT is typically restricted to presynaptic terminals of neurons emanating from the raphe, and thus, rat cortical neurons do not express significant levels of the transporter (40,41). Embryonic rat cortical neurons were electroporated with an EYFP-tagged SERT construct under the control of the CaMKII promoter to restrict expression to excitatory pyramidal neurons. Sparse transfection resulted in cultures expressing both SERT-positive and SERT-negative neurons (Fig. 4B), enabling us to compare the effects of serotonin on neurons capable of importing the monoamine to those that could not within the same cultures.

Treatment with the membrane permeable psychedelic DMT (10 μM) resulted in greater dendritic arbor complexity and increased spine density in both SERT-positive and SERT-negative neurons (Fig. 4B–F). Only SERT-positive neurons treated with serotonin (10 μM) displayed increased dendritogenesis and spinogenesis (Fig. 4B–F). To ensure that serotonin-induced changes in structural neural plasticity were due to engagement of intracellular 5-HT2Rs via serotonin importation from SERT, we performed similar experiments in the presence of the selective SERT inhibitor citalopram (CIT) and KTSN. When these experiments were performed in the presence of CIT (10 μM), the plasticity-promoting effects of serotonin (1 μM) on SERT-positive neurons were blocked (Fig. 4D). In contrast, CIT had no effect on the ability of DMT (1 μM) to promote the growth of SERT-positive or SERT-negative cortical neurons (Fig. 4D). In the presence of KTSN (10 μM), neither serotonin nor DMT could promote neuronal growth, confirming that DMT and intracellular serotonin promote plasticity via 5-HT2AR receptors in vitro (Fig. 4D).

To determine if intracellular serotonin could promote the growth of cortical neurons in vivo, we injected the medial PFC (mPFC) of Thy1-EGFP mice with either CaMKII-SERT-mCherry or CaMKII-mCherry. The mPFC was chosen as the injection site because it exhibits high levels of 5-HT2AR expression (28) and has been implicated in the antidepressant-like effects of psychoplastogens (42). After 3 weeks to enable construct expression (Fig. 5A and B), both groups were administered (±)-para-chloroamphetamine (PCA, 5 mg/kg, IP)—a selective serotonin-releasing agent (43). Dendritic spine density on mPFC pyramidal neurons was assessed 24 h later. Animals expressing SERT in the mPFC displayed significantly higher densities of dendritic spines following PCA administration as compared to mCherry controls (Fig. 5C and D). Importantly, PCA is not a 5-HT2AR agonist (fig. S10A), does not directly promote the growth of SERT-positive or SERT-negative cortical neurons in culture (fig. S10B), and does not induce a HTR in wild type mice (fig. S10C).

Evidence suggests that psychoplastogen-induced structural plasticity in the mPFC might be related to sustained antidepressant-like effects in rodents (44). To probe for an antidepressant-like response that might be linked to neuroplasticity, we injected an AAV containing a CaMKII-SERT-EYFP or CaMKII-GFP construct into the mPFC of wild type C57BL/6J mice (Fig. 5E and fig. S10D). After 3 weeks to allow for construct expression, both groups of mice underwent a novelty induced locomotion (NIL) test and no differences in locomotion were observed (Fig. 5F). After 24 h, mice were subjected to a forced swim test (FST) (7,45). Again, we observed no differences between the mice expressing SERT

and those expressing the GFP control (Fig. 5G). Two days later, we administered PCA (5 mg/kg, IP), waited 24 h, and then performed a second FST (Fig. 5G). The SERT-expressing mice exhibited a statistically significant HTR immediately following the administration of PCA as compared to the GFP control mice (fig. S10E), and they also displayed a significant reduction in immobility 24 h post administration (Fig. 5G).

DISCUSSION

Though GPCRs are traditionally viewed as initiators of signal transduction originating at the plasma membrane, increasing evidence suggests that GPCR signaling from intracellular compartments can play important roles in cellular responses to drugs. Recently, location bias has been proposed to explain signaling differences between endogenous membrane-impermeable peptide ligands and membrane-permeable ligands of opioid receptors (38). Moreover, distinct ligand-induced signaling has been observed for plasma membrane-localized and intracellular populations of δ-opioid receptors (46). Here, we extend the concept of location bias to ligands of the 5-HT2AR.

Given that a substantial proportion of 5-HT2ARs in cortical neurons are localized to the Golgi and intracellular compartments like the Golgi are slightly acidic compared to the cytosol and extracellular space, it is possible that protonation of psychedelics within the Golgi leads to retention and sustained signaling resulting in neuronal growth, even after transient stimulation (47). Persistent growth after the drugs have been removed from the extracellular space is a hallmark of serotonergic psychoplastogens (47,48). While the mechanistic details linking intracellular 5-HT2AR activation to cortical neuron growth have not been fully elucidated, they are likely to involve AMPA receptor, TrkB, and mTOR signaling as previously established (9). Future studies should examine the detailed signaling interplay between these proteins.

In addition to promoting psychedelic-induced structural neuroplasticity, the intracellular population of 5-HT2ARs might also contribute to the hallucinogenic effects of psychedelics. When we administered a serotonin-releasing agent to wild type mice, we did not observe a HTR. However, the same drug was able to induce a HTR in mice expressing SERT on cortical neurons of the mPFC—a brain region known to be essential for the HTR (49). Thus, activation of intracellular cortical 5-HT2ARs may play a role in the subjective effects of psychedelics. This hypothesis is further supported by previous work demonstrating that a high dose of the serotonin precursor 5-hydroxytryptophan (5-HTP) induces a HTR in WT mice, which can be blocked by an *N*-methyltransferase inhibitor that prevents the metabolism of 5-HTP to *N*-methyltryptamines (50). Inhibition of *N*-methyltransferase failed to block the HTR induced by 5-MeO-DMT (50). Taken together, this work emphasizes that accessing intracellular 5-HT2ARs is important for 5-HT2AR agonists to produce a HTR.

Our results demonstrate that membrane permeability is essential for a ligand to activate 5-HT2ARs in cortical neurons; however, our experiments did not distinguish between intracellular signaling or the possibility of psychedelics acting as pharmacological chaperones. Others have hypothesized that GPCR ligands may act as pharmacological chaperones, facilitating their export to the plasma membrane where they could presumably

engage in canonical signaling (53). Thus, future studies should determine if intracellular 5-HT2AR signaling is distinct from 5-HT2AR signaling at the plasma membrane.

While intracellular expression of 5-HT2ARs within cortical pyramidal neurons has been known for some time, it is currently unclear why the subcellular localization of these receptors differs greatly between neurons and HEK293T cells (28,29,31). One possibility is that 5-HT2ARs form heterodimeric complexes that impact cellular trafficking (31). Thus, by dictating 5-HT2AR localization, cellular context could influence responses to endogenous neuromodulators and/or exogenous drugs, potentially resulting in circuit-specific effects of 5-HT2AR ligands.

Intracellular signaling has been hypothesized to contribute to the pharmacological properties of a diverse range of compounds including nicotine, ketamine, and SSRIs (51,52,53). Like psychedelics, these compounds are weak bases with pKa values ranging from 7–10. Given that the antidepressant mechanisms of ketamine and SSRIs have not been definitively established, it is intriguing to speculate that they too might promote cortical neuron growth by binding to intracellular targets. Perhaps other antidepressants impact the function of scaffolding proteins within the cell interior to modulate neuronal growth phenotypes.

Without facilitated transport across the plasma membrane, serotonin cannot induce psychedelic-like effects on neuronal morphology. While it is possible that 5-HT could alter cortical neuron physiology by activating cell surface 5-HT2ARs, this receptor pool does not seem to be involved in 5-HT2AR-induced structural plasticity. Our results raise the intriguing possibility that serotonin may not be the endogenous ligand for the population of 5-HT2ARs expressed inside cortical neurons. Alternative ligands could include methylated analogs of serotonin or tryptamine, because these compounds possess greater abilities to cross nonpolar membranes. Endogenous psychedelics such as DMT, 5-MeO-DMT, and bufotenin have been identified in a variety of species including humans and have long been hypothesized to play roles in diseases like schizophrenia (54). However, they are rapidly degraded in vivo, making their detection by classic analytical methods quite challenging. The use of more modern analytical techniques has improved detection of these analytes (55), with a recent study demonstrating that the concentration of DMT in the cortex was comparable to that of serotonin (56). The possibility of endogenous psychedelics playing a role in health or disease should therefore be thoroughly investigated.

Supplementary Material

Refer to Web version on PubMed Central for supplementary material.

Acknowledgements:

General.

We thank Calvin Ly, Alexandra C. Greb, Lindsay P. Cameron, and Whitney C. Duim for performing early pilot studies, Arabo Avanes for assistance with radioligand binding studies, Karen Zito for providing Thy1-GFP breeders, Javier González-Maeso for providing the Myc-5-HT2AR-ECFP plasmid, Rishab Iyer for performing HRMS analysis, and Peter Beal for use of his CLARIOStar plate reader. We also thank Charles Nichols for advice about the radioligand binding experiments.

Funding.

This work was supported by funds from the National Institutes of Health (NIH) (R01GM128997 to DEO; R35GM133421 to JDM, and U01NS120820, U01NS115579, 2R01MH101214-06 to LT), three NIH training grants (T32GM099608 to MVV; T32GM113770 to RJT; and T32MH112507 to HNS), Human Frontier (LT), the Camille and Henry Dreyfus Foundation (DEO), a sponsored research agreement with Delix Therapeutics (DEO), and a UC Davis Provost's Undergraduate Fellowship (SC). This project used the Biological Analysis Core of the UC Davis MIND Institute Intellectual and Development Disabilities Research Center (U54 HD079125). The Nikon High Content Analysis Spinning Disk Confocal microscope used in this study was purchased using NIH Shared Instrumentation Grant 1S10OD019980-01A1. We thank the MCB Light Microscopy Imaging Facility, which is a UC Davis Campus Core Research Facility, for the use of this microscope. Funding for the NMR spectrometers was provided by the National Science Foundation (#NSF CHE-04-43516) and National Institutes of Health (#08P0ES 05707C). Analysis for this project was performed in the UC Davis Campus Mass Spectrometry Facilities with instrument funding provided by the NIH (1S10OD025271-01A1). Several of the drugs used in this study were provided by the NIDA Drug Supply Program.

Data and materials availability.

Data are available at the following link: https://doi.org/10.6084/m9.figshare.21669635. Custom written data analysis codes are available via GitHub (see methods for details). All materials are available upon request or commercially available. TMT and MKTSN are available from David E. Olson and psychLight is available from Lin Tian under material agreements with the University of California, Davis.

References and Notes:

1. Duman RS, Aghajanian GK, J. H. G. & Krystal, Nat. Med. 22, 238–49 (2016). [PubMed: 26937618]
2. Qiao H et al., Neural Plast. 2016, 8056370 (2016). [PubMed: 26881133]
3. Shansky RM, Hamo C, Hof PR, McEwen BS, Morrison JH, Cereb. Cortex 10, 2479–84 (2009).
4. Rantamäki T et al., Neuropsychopharmacology 32, 2152–62 (2007). [PubMed: 17314919]
5. Casarotto PC et al., Cell 184, 1299–313 (2021). [PubMed: 33606976]
6. Olson DE, J. Exp. Neurosci. 12,1179069518800508 (2018). [PubMed: 30262987]
7. Vargas MV, Meyer R, Avanes AA, Rus M, Olson DE, Front. Psychiatry 12, 727117 (2021). [PubMed: 34671279]
8. Kwan AC, Olson DE, Preller KH, Roth BL, Nat. Neurosci. 25, 1407–1419 (2022) [PubMed: 36280799]
9. Ly C et al., Cell Rep. 11, 3170–3182 (2018).
10. de la Fuente Revenga M et al., Cell Rep. 37, 109836 (2021). [PubMed: 34686347]
11. Olson DE, Biochemistry 61, 27–136 (2021).
12. Dunlap LE et al., J. Med. Chem. 63, 1142–1155 (2020). [PubMed: 31977208]
13. Cameron LP et al., Nature 589, 474–479 (2021). [PubMed: 33299186]
14. Dong C et al., Cell 184, 2779–2792.e18 (2021). [PubMed: 33915107]
15. Cao D et al., Science 375, 403–411(2022). [PubMed: 35084960]
16. Luttrell LM, Maudsley S, Bohn LM, Mol. Pharmacol. 88, 579–88 (2015). [PubMed: 26134495]
17. Kim K et al., Cell 182, 1574–1588 (2020). [PubMed: 32946782]
18. Irannejad R et al., Nat. Chem. Biol. 13, 799–806 (2017). [PubMed: 28553949]
19. Mohammad MA, Nezhady, Rivera JC, Chemtob S, iScience 23, 101643 (2020). [PubMed: 33103080]
20. Weisstaub NV et al. Science 313, 536–540 (2006). [PubMed: 16873667]
21. Ristanović D, Milosević NT, Stulić V, Neurosci J. Methods 2, 212–8 (2006).
22. Ebersole BJ, Visiers I, Weinstein H, Sealfon SC, Mol. Pharmacol. 63, 36–43 (2003). [PubMed: 12488534]
23. Olsen RHJ et al., Nat. Chem. Biol. 16, 841–849 (2020). [PubMed: 32367019]

24. Bermak JC, Li M, Bullock C, Zhou QY, Nat. Cell Biol. 3, 492–8 (2001). [PubMed: 11331877]
25. Petaja-Repo UE, Hogue M, Laperriere A, Walker P, Bouvier M, J. Biol. Chem. 275, 13727–36 (2000). [PubMed: 10788493]
26. Jacobsen SE et al. J. Biol. Chem. 292, 6910–6926 (2017). [PubMed: 28280242]
27. Purgert CA et al., J. Neurosci. 34, 4589–4598 (2014). [PubMed: 24672004]
28. Cornea-Hébert V, Riad M, Wu C, Singh SK, Descarries L, J. Comp. Neurol. 409, 187–209 (1999). [PubMed: 10379914]
29. Cornea-Hébert V et al., Neuroscience 113, 23–35 (2002). [PubMed: 12123681]
30. Schmid CL, Raehal KM, Bohn LM, Proc. Natl. Acad. Sci. U.S.A. 105, 1079–84 (2008). [PubMed: 18195357]
31. Toneatti R et al., Sci. Signal 13, 654 (2020).
32. Saffitz JE, Liggett SB, Circ. Res. 70, 1320–5 (1992). [PubMed: 1315641]
33. Fu Q, Xiang YK, Prog. Mol. Biol. Transl. Sci. 132,151–88 (2015). [PubMed: 26055058]
34. Magalhaes AC et al., Nat. Neurosci. 13, 622–9 (2010). [PubMed: 20383137]
35. Seachrist JL, Ferguson SS, Life Sci. 74, 225–35 (2003). [PubMed: 14607250]
36. Nash CA, Wei W, Irannejad R, Smrcka AV, Elife 8, e48167 (2019). [PubMed: 31433293]
37. Irannejad R et al., Nature 495, 534–8 (2013). [PubMed: 23515162]
38. Stoeber M et al., Neuron 98, 963–976 (2018). [PubMed: 29754753]
39. Aggarwal S, Mortensen OV, Curr. Protoc. Pharmacol. 79, 12.16.1–12.16.17 (2017).
40. Zhou FC, Sari Y, Zhang JK, Brain Res. Dev. Brain Res. 119, 33–45 (2000). [PubMed: 10648870]
41. Lebrand C et al., J. Comp. Neurol. 401, 506–24 (1998). [PubMed: 9826275]
42. Fuchikami M et al., Proc. Natl. Acad. Sci. U. S. A. 112, 8106–11 (2015). [PubMed: 26056286]
43. Sharp T, Zetterström T, Christmanson L, Ungerstedt U, Neurosci. Lett. 72, 320–4 (1986). [PubMed: 3822235]
44. Moda-Sava RN et al., Science 364, eaat8078 (2019). [PubMed: 30975859]
45. Slattery DA, Cryan JF, Nat. Protoc. 7, 1009–14 (2012). [PubMed: 22555240]
46. Crilly SE, Ko W, Weinberg ZY, Puthenveedu MA, Elife 2021, e67478 (2021).
47. Ly C et al., A.C.S. Pharmacol. Transl. Sci. 4, 452–460 (2020).
48. Shao LX et al., Neuron 109, 2535–2544 (2021). [PubMed: 34228959]
49. González-Maeso J et al., Neuron 53, 439–452 (2007). [PubMed: 17270739]
50. Schmid CL, Bohn LM, J Neurosci. 40, 13513–24 (2010).
51. Henderson BJ, Lester HA, Neuropharmacology 96, 178–93 (2015). [PubMed: 25660637]
52. Lester HA, Lavis LD, Dougherty DA, Am. J. Psychiatry 172, 1064–6 (2015). [PubMed: 26183700]
53. Lester HA, Miwa JM, Srinivasan R, Biol. Psychiatry 72, 907–915 (2012). [PubMed: 22771239]
54. Barker SA, McIlhenny EH, Strassman R, Drug Test Anal 7–8, 617–35 (2012).
55. Barker SA, Borjigin J, Lomnicka I, Strassman R, Biomed. Chromatogr. 27, 1690–700 (2013). [PubMed: 23881860]
56. Dean JG et al., Sci. Rep. 9, 9333 (2019). [PubMed: 31249368]
57. Toneatti R et al., Sci. Signal 13, eaaw3122 (2020). [PubMed: 33082287]
58. McCall J, Nicholson L, Weidner N, Blesch A, Front. Mol. Neurosci. 2012, 5:11 (2012).
59. Bradford MM, Anal. Biochem. 72, 248–254 (1976). [PubMed: 942051]

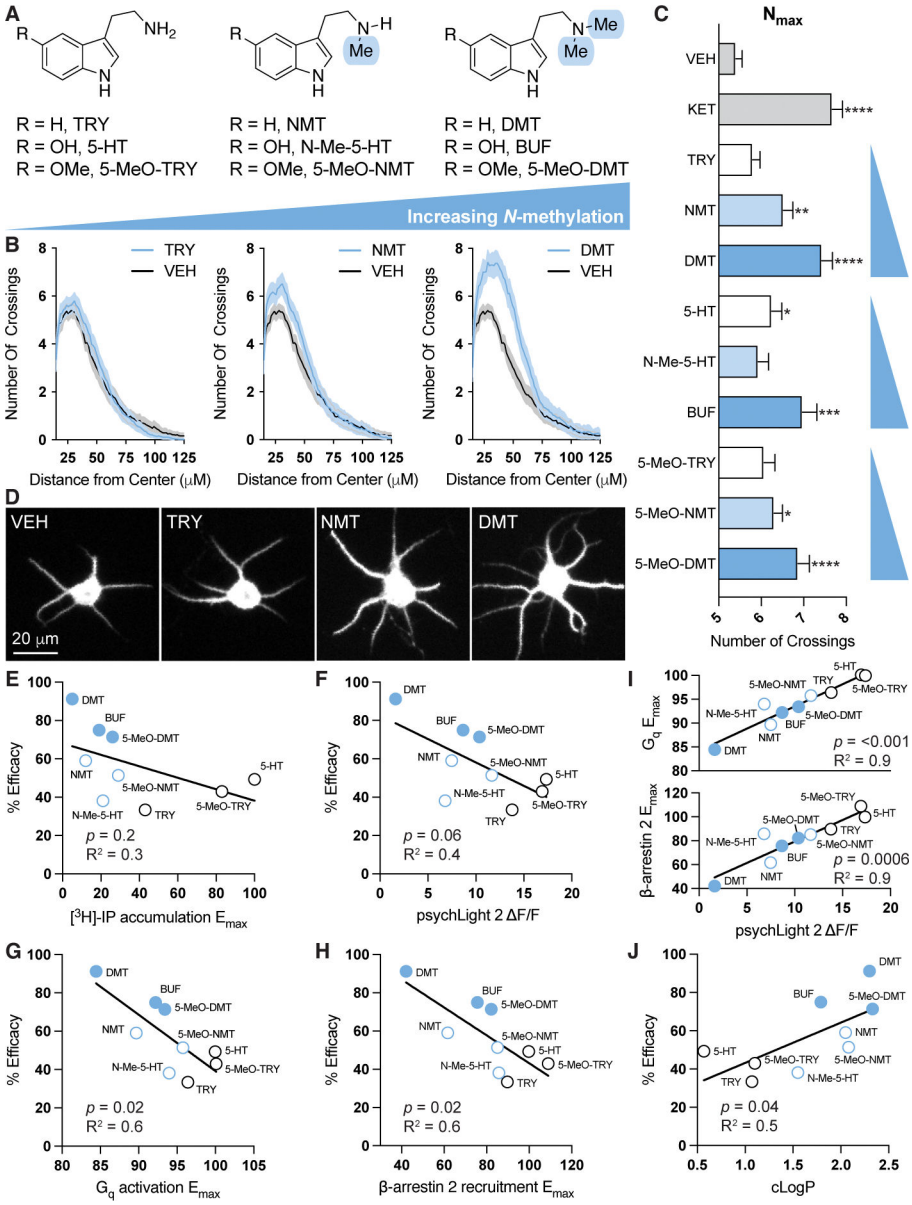

Fig. 1. Compound-Induced Neuronal Growth Correlates with Ligand Lipophilicity.

(**A**) Chemical structures of serotonin, tryptamine, and 5-MeO-tryptamine as well as their corresponding *N*-methyl and *N,N*-dimethyl analogs. (**B**) Sholl analysis demonstrates that increasing *N*-methylation leads to a concomitant increase in dendritic arbor complexity. The shaded area represents 95% confidence intervals. Sholl plots were generated from rat embryonic cortical neurons (DIV6) treated with compounds (10 μM). (**C**) Maximum numbers of crossings (N_{max}) of the Sholl plots in B (N = 45–64 neurons per treatment). (**D**) Images of rat embryonic cortical neurons (DIV6) treated with compounds (10 μM). (**E**–**J**) Correlation plots of Sholl analysis % efficacy (N_{max} values relative to 10 μM ketamine as the positive control) vs [^{3}H]-IP accumulation (E), activation of psychLight2 (F), G_q activation (G), β-arrestin recruitment (H), or calculated LogP (J). PsychLight2 activation correlates well with both G_q activation and β-arrestin recruitment (I). Compounds treated

at 10 μM. Data for [^{3}H]-IP accumulation was obtained from literature values (22). VEH = vehicle, KET = ketamine, TRY = tryptamine, NMT = *N*-methyltryptamine, DMT = *N,N*-dimethyltryptamine, 5-HT = serotonin, N-Me-5-HT = *N*-methylserotonin, BUF = bufotenin, 5-MeO-TRY = 5-methoxytryptamine, 5-MeO-NMT = 5-methoxy-*N*-methyltryptamine, 5-MeO-DMT = 5-methoxy-*N,N*-dimethyltryptamine. *p < 0.05, **p < 0.01, ***p < 0.001, ****p < 0.0001, as compared to VEH controls (one-way ANOVA followed by Dunnett's multiple comparisons test). R^2 values calculated via simple liner regression.

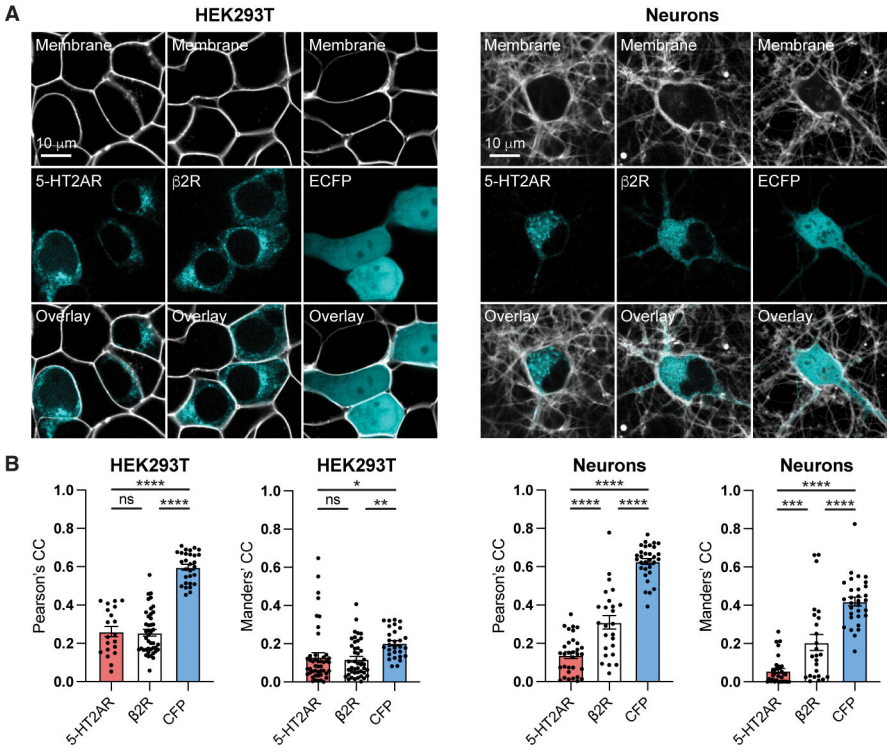

Fig. 2. Cortical neurons express intracellular 5-HT2A receptors.

(**A**) Live cell images of HEK293T cells and rat embryonic cortical neurons (DIV6) expressing Myc-5-HT2AR-CFP, β2AR-ECFP, or ECFP. Signals from the fluorescent protein and fluorescent plasma membrane marker (Cellbrite® Steady) are shown in cyan and white, respectively. The expression patterns of 5-HT2ARs and β2ARs are comparable in HEK293T cells. However, in neurons, β2ARs exhibit higher expression on the plasma membrane than 5-HT2ARs. The expression of ECFP is diffuse in both HEK293T cells and cortical neurons. (**B**) Pearson's Correlation Coefficient (PCC) and Manders' Colocalization Coefficients (MCC) quantify the extent of colocalization between MYC-5-HT2AR-CFP, β2AR-ECFP, or ECFP and the fluorescent plasma membrane marker (N = 20–43 cells per group). ECFP = enhanced cyan fluorescent protein. *p < 0.05, **p < 0.01, ***p < 0.001, ****p < 0.0001, bars indicate comparisons between data (one-way ANOVA followed by Tukey's multiple comparisons test).

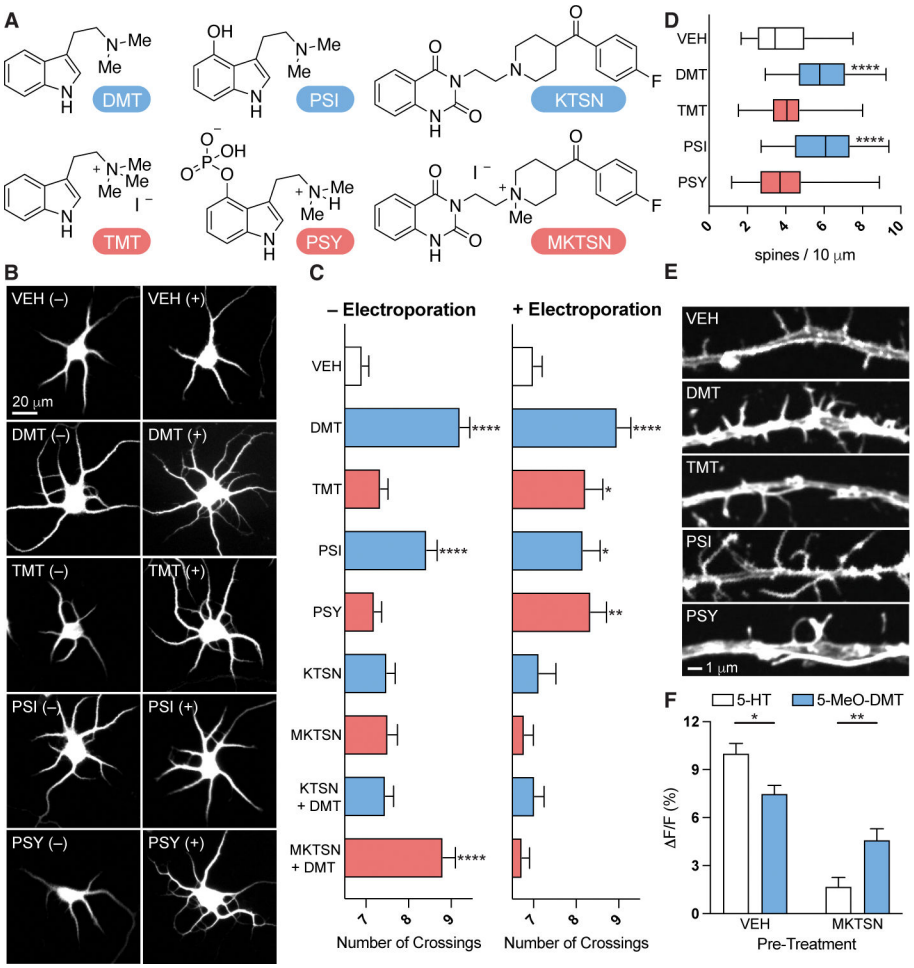

Fig. 3. Intracellular 5-HT2ARs mediate structural plasticity induced by serotonergic psychoplastogens.

(**A**) Structures of membrane permeable (blue) and impermeable (red) compounds. (**B**) Images of rat embryonic cortical neurons (DIV6) administered compounds with (+) and without (–) electroporation. (**C**) N_{max} values obtained from Sholl plots. Membrane impermeable analogs of psychedelics (1 μM) only promote growth when administered with electroporation (N = 35–110 neurons per treatment). Unlike KTSN (10 μM), MKTSN (10 μM) only blocks psychedelic-induced plasticity when administered with electroporation (N = 45–109 neurons per treatment). (**D**) Membrane impermeable agonists of 5-HT2ARs (1 μM) cannot promote spinogenesis in cultured embryonic rat cortical neurons (DIV15) (N = 30–34 neurons per treatment). (**E**) Images of treated cortical neurons (DIV15). (**F**) HEK293T cells expressing psychLight1 were pretreated with VEH or MKTSN (10 μM) prior to the administration of 5-HT (10 μM) or 5-MeO-DMT (10 μM). (N = 41–54 cells per treatment). $p < 0.05$, $^{**}p < 0.01$, $^{***}p < 0.001$, $^{****}p < 0.0001$, as compared to VEH controls in (D) and (C) (one-way ANOVA followed by Dunnett's multiple comparisons test), or between indicated pairs of data in (F) (two-way ANOVA followed by Šídák's multiple comparisons test). For box-and-whisker plots, center line = median; box limits = upper and lower quartiles; whiskers = min and max values.

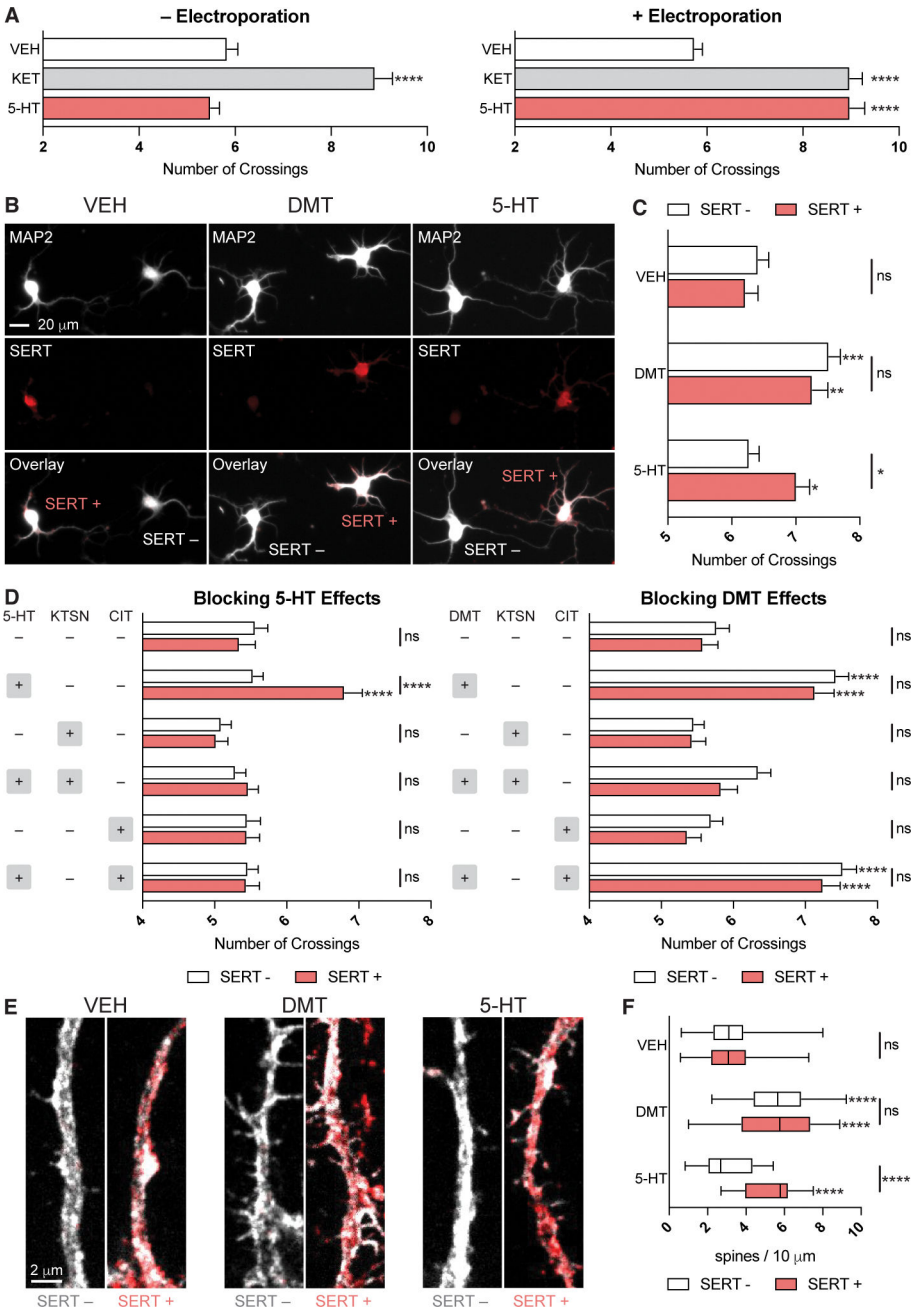

Fig. 4. Cellular uptake of 5-HT induces structural plasticity in vitro.

(**A**) Rat embryonic cortical neurons were administered compounds (1 μM) with (+) and without (–) electroporation. N_{max} values obtained from Sholl plots (DIV6) demonstrates that unlike ketamine, serotonin only promotes growth when administered with electroporation (N = 49–59 neurons per treatment). (**B**) Images of embryonic rat cortical cultures (DIV6) sparsely transfected with CaMKII-SERT-EYFP and treated with compounds. (**C**) N_{max} values obtained from Sholl plots demonstrate that 5-HT (10 μM) can only increase the dendritic arbor complexity of SERT+ neurons, while DMT (10 μM) can promote the growth of both SERT+ and SERT– neurons (N = 69–93 neurons per treatment). (**D**) KTSN

pretreatment (10 μM) blocks the plasticity-promoting effects of 5-HT (1 μM) in SERT+ neurons and DMT (1 μM) in both SERT+ and SERT– neurons. CIT (10 μM) only blocks the plasticity-promoting effects of 5-HT (1 μM) in SERT+ neurons (N = 59–100 neurons per treatment). (**E**) Images of CaMKII-SERT-EYFP positive and negative dendrites (DIV15) treated with compounds (10 μM). (**F**) 5-HT only promotes spine growth in SERT+ neurons (N = 11–35 neurons per treatment). *p < 0.05, **p < 0.01, ***p < 0.001, ****p < 0.0001, as compared to VEH controls in (A) (one-way ANOVA followed by Dunnett's multiple comparisons test), or compared to VEH controls from the same genotype in (C), (D), and (F) (two-way ANOVA followed by Tukey's multiple comparisons test). For box-and-whisker plots, center line = median; box limits = upper and lower quartiles; whiskers = min and max values.

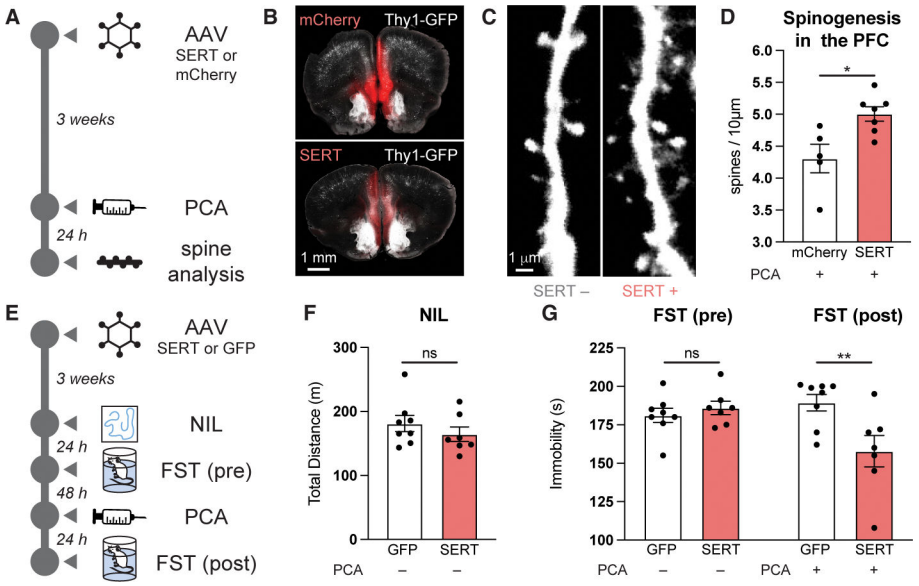

Fig. 5. Cellular uptake of 5-HT produces antidepressant-like effects in vivo.

(**A**) Schematic displaying experimental design for measuring spine density in Thy1-EGFP mice following administration of a serotonin-releasing agent. (**B**) Histology images of Thy1-EGFP mice expressing CaMKII-mCherry or CaMKII-SERT-mCherry in the mPFC. (**C**) Images of dendritic spines in the mPFC of mice treated with PCA (5 mg/kg, IP). (**D**) Mice expressing CaMKII-SERT-mCherry display increased dendritic spine density following PCA treatment. (**E**) Schematic displaying experimental design for determining the sustained antidepressant-like effects of serotonin in mice expressing SERT in the mPFC. (**F**) NIL demonstrates no difference between CaMKII-SERT-EYFP and CaMKII-GFP expressing mice. (**G**) CaMKII-SERT-EYFP and CaMKII-GFP expressing mice exhibit no differences in the FST. After PCA (5 mg/kg, IP) administration, CaMKII-SERT-EYFP expressing mice display a sustained antidepressant-like effect. *$p < 0.05$, **$p < 0.01$, ***$p < 0.001$, ****$p < 0.0001$, as compared between indicated pairs of data in (D) and (F) (two-tailed unpaired Student's *t* test), or (G) (two-way repeated measures ANOVA followed by Šídák's multiple comparisons test. For box-and-whisker plots, center line = median; box limits = upper and lower quartiles; whiskers = min and max values.